IN SITU ANALYSIS OF ORTHOPYROXENE IN DIOGENITES USING LASER ABLATION ICP-MS.

M. Ek[1], J. E. Quinn[2], D. W. Mittlefehldt[3], [1]Department of Earth Sciences, University of Gothenburg, Sweden (mattias.ek@student.gu.se), [2]Jacobs Engineering, ESCG, Houston, TX, USA; current: PANalytical, Inc., Westborough, MA, USA, [3]Astromaterials Research Office, NASA/Johnson Space Center, Houston, TX, USA.

Introduction: Howardites, eucrites and diogenites (HED) form a suit of igneous achondrite meteorites that are thought to have formed on a single asteroidal body. While there have been many different models proposed for the formation of the HED parent asteroid they can be generalized into two end member models. One is the magma ocean model (e.g. [1]) in which the entire HED parent body was continuously fractionated from a planet wide magma ocean with diogenites representing the lower crust and eucrites being upper crustal rocks. The second model hypothesizes that diogenites and eucrites were formed as a series of intrusions and/or extrusions of partial melts of a primitive proto-Vesta [2]. We use in situ trace element analysis together with major and minor element analysis to try and distinguish between these different hypotheses for the evolution of the HED parent body.

Method: Major and minor element compositions of orthopyroxene and olivine grains were determined using a Cameca SX100 electron microprobe at JSC using a 20 kv accelerating voltage and 40 na beam current. In situ trace element compositions were analysed using a New Wave Research 193 nm solid state Nd:YAG laser ablation unit connected to a Thermo Scientific Element-XR magnetic sector ICP-MS at JSC. Analyses were carried out using a 100 micron spot size, 10Hz repetition rate and 100% laser output. All elements were measured in low resolution mode and Ca43 was used as an internal standard to calculate absolute concentrations. The USGS standard glasses BIR1g, BVHO2g, and BCR2g were used to calculate calibration lines. The precision is estimated to be better than ±10% for all elements apart from Sr, La and Eu; due to their low concentrations their precision is estimated to be better than ±20%.

Results: Compositions of orthopyroxene and olivine grains were determined for core compositions and for zoning against adjacent minor minerals. These results were used to select targets for trace element analysis. Brief petrological descriptions and analytical results follow.

SAN 03473,13 is a brecciated diogenite containing small amounts of accessory silica and metal phases. Orthopyroxene has an Mg# of 76.8-77.4 and a Fe/Mn ratio of 26-28. The minor element variations are large compared to the other diogenites and the distribution is scattered and does not follow linear trends (Fig. 1) as is commonly observed in diogenites [3]. Trace elements show a similar scattering (Fig. 1). Most orthopyroxenes have a Eu/Eu* value of 0.18-0.23 with another possible cluster of 0.35-0.40. (Eu* is the Eu content inferred from REE patterns.)

GRA 98108,30 is an unbrecciated harzburgitic diogenite with a high olivine content (~18%) [4] and an orthopyroxene Mg# of 76.7. The minor and trace element variations are small and clustered (Fig. 1). It has a low Eu/Eu* ratio of 0.04-0.12, together with a strong LREE depletion.

GRO 95555,47 is an unbrecciated diogenite containing small amounts of silica in close association

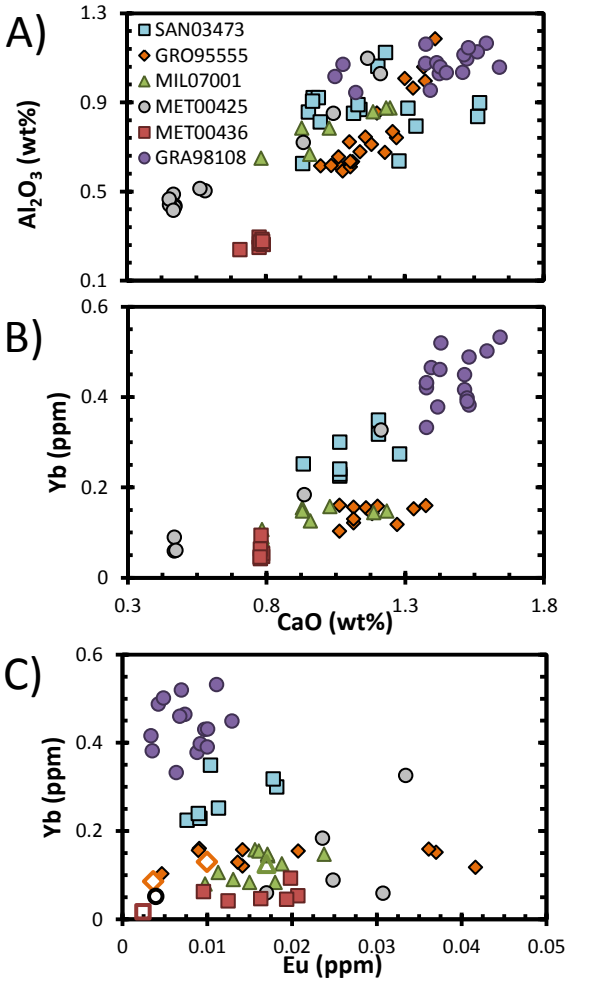

Figure 1. A) Al2O3 *vs.* CaO for orthopyroxene from EMPA analyses. B) Yb *vs.* CaO for the laser ablation analyses. C) Yb *vs.* Eu for the analyses in B. The unfilled points indicate values from [5, 6] for MIL 07001, MET 00425, MET 00436 and GRO 95555.

with a metal phase (Fig. 2). Orthopyroxene has an Mg# of 75.5. Minor element compositions show significant linear variations (Fig. 1), with higher concentrations closer to the silica inclusions (Fig. 2). The trace elements show a similar trend. The Eu/Eu* ratio is 0.4-0.7 and the REE concentrations are similar to those from [5, 6].

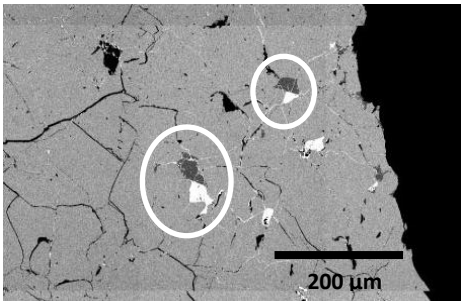

Figure 2. Backscatter image of GRO95555, 47 showing the silica phase in association with a metal phase. The white rings indicate where the highest concentrations of incompatible elements can be found.

MIL 07001,40 is an unbrecciated harburgitic diogenite. Orthopyroxene has a Mg# of 76.5. Olivine occurs as small rounded grains poikilitically included in orthopyroxene. There are small variations in the minor and trace element concentrations in orthopyroxene that follow a linear trend (Fig. 1). The REE concentrations and Eu/Eu* ratios of 0.5-0.7 are similar to those a bulk rock analysis from [5].

MET 00425,23 is a brecciated diogenite containing silica in contact with orthopyroxene. There are two populations of orthopyroxene. One has an Mg# number of 83.5, and a low narrow range of minor and trace elements concentrations (Fig. 1). The other has an Mg# of ~81 with a large span of minor and trace element concentrations that follow linear trends (Fig. 1). The second population appears to be associated with orthopyroxene in contact with silica. The orthopyroxene Eu/Eu* ratios vary between 0.3-0.7.

MET 00436,35 is an unbrecciated diogenite containing large chromite grains. The Mg# for orthopyroxene in this sample is low at ~70-71. Minor and trace element concentrations are low with narrow ranges (Fig. 1) and the Eu/Eu* ratio is 0.5-0.8.

Discussion: The major and minor element compositions of the diogenites analyzed here are within the ranges of other diogenites [3]. Increases in concentrations of minor and trace elements within GRO 95555 and MET 00425 are linked to their proximity to a silica phase (Fig. 2). This suggests that the silica phase and adjacent pyroxene was formed from a more compositionally evolved magma and/or interacted with interstitial melt. This is also suggested by the association of higher minor element concentrations with more Fe-rich orthopyroxene in MET 00425. The correlation of Al_2O_3 and CaO appears to be linear in all diogenites except SAN 03473, suggesting that the geologic history of this diogenite is more complex.

There is a clear relationship between the minor and trace element concentrations in diogenites, apart from Sr and Eu. While these elements can be correlated with minor element concentrations within individual diogenites, there is no cross sample trend as observed for the other elements. This suggests that the diogenites did not form from a single fractionation sequence. This is also supported by the wide range of concentrations of trace elements observed. If all diogenites formed from the same fractionation sequence, then the magma chamber would have to have undergone 70-90% of perfect fractionational crystallization to create the range in incompatible trace element concentrations. This is inconsistent with the small range of Mg# observed in orthopyroxene; if a magma chamber undergoes 70-90% fractionation then one would expect a very low Mg# in orthopyroxene with high incompatible element contents. A more plausible scenario is that the diogenites formed from multiple magma chambers with different initial composition [7]. However, it is unclear how different diogenite parent magmas acquired vastly different trace element contents, although the magma contamination model [3] is one possibility. This favors the idea that diogenites may have formed from chemically distinct magmas rather than a single, asteroid-wide magma ocean.

The REE concentrations and Eu/Eu* ratios calculated for GRO95555, MIL07001 and MET00425 agree well with those obtained from previous studies [5, 6], although the concentrations obtained in this study are a factor of 1-5 higher than the previous studies for some diogenites. This difference may reflect heterogeneity in the diogenites (e.g. [8]). We find MET00436 is more LREE depleted than determined by [5] in addition to having up to a factor of 10 higher concentrations for the mid to high REE's, again, suggesting possible heterogeneity.

References: [1] Righter, K. & Drake, M.J. (1997) *Meteoritics & Planet. Sci.*, 32, 929-944. [2] Stolper, E. (1977) *Geochim. Cosmochim. Acta*, 41, 587-611. [3] Mittlefehldt, D.W. (1994) *Geochim. Cosmochim. Acta*, 58, 1537-1552. [4] Beck, A.W. & McSween H.Y. Jr. (2010) *Meteoritics & Planet. Sci.*, 45, 850-872. [5] Barrat, J.-A. et al. (2010) *Geochim. Cosmochim. Acta*, 74, 6218-6231. [6] Papike, J.J. et al. (2000) *Meteoritics & Planet. Sci.*, 35, 875-879. [7] Shearer, C.K. et al. (1997) *Meteoritics & Planet. Sci.*, 32, 877-889. [8] Fowler, G.W. et al. (1995) *Geochim. Cosmochim. Acta*, 59, 3071-3084.